BJP British Journal of Pharmacology

DOI:10.1111/bph.12100
www.brjpharmacol.org

RESEARCH PAPER

Effects of hydrogen sulphide on motility patterns in the rat colon

V Gil[1,2], SP Parsons[2], D Gallego[3], JD Huizinga[2] and M Jimenez[1,3]

[1]*Department of Cell Biology, Physiology and Immunology/Neuroscience Institute, Universitat Autònoma de Barcelona (UAB), Barcelona, Spain,* [2]*Department of Medicine, Farncombe Family Digestive Health Research Institute, McMaster University, Hamilton, ON, Canada, and* [3]*Centro de Investigación Biomédica en Red de Enfermedades Hepáticas y Digestivas (CIBEREHD), Instituto de Salud Carlos III, Barcelona, Spain*

Correspondence
Marcel Jimenez, Department of Cell Biology, Physiology and Immunology, Universitat Autònoma de Barcelona (UAB), 08193 Bellaterra, Barcelona, Spain. E-mail: marcel.jimenez@uab.es

Keywords
hydrogen sulphide; neuromuscular transmission; IJP; EJP; motility; smooth muscle; gastrointestinal

Received
10 July 2012
Revised
26 November 2012
Accepted
17 December 2012

BACKGROUND AND PURPOSE
Hydrogen sulphide (H_2S) is an endogenous gaseous signalling molecule with putative functions in gastrointestinal motility regulation. Characterization of H_2S effects on colonic motility is crucial to establish its potential use as therapeutic agent in the treatment of colonic disorders.

EXPERIMENTAL APPROACH
H_2S effects on colonic motility were characterized using video recordings and construction of spatio-temporal maps. Microelectrode and muscle bath studies were performed to investigate the mechanisms underlying H_2S effects. NaHS was used as the source of H_2S.

KEY RESULTS
Rhythmic propulsive motor complexes (RPMCs) and ripples were observed in colonic spatio-temporal maps. Serosal addition of NaHS concentration-dependently inhibited RPMCs. In contrast, NaHS increased amplitude of the ripples without changing their frequency. Therefore, ripples became the predominant motor pattern. Neuronal blockade with lidocaine inhibited RPMCs, which were restored after administration of carbachol. Subsequent addition of NaHS inhibited RPMCs. Luminal addition of NaHS did not modify motility patterns. NaHS inhibited cholinergic excitatory junction potentials, carbachol-induced contractions and hyperpolarized smooth muscle cells, but did not modify slow wave activity.

CONCLUSIONS AND IMPLICATIONS
H_2S modulated colonic motility inhibiting propulsive contractile activity and enhancing the amplitude of ripples, promoting mixing. Muscle hyperpolarization and inhibition of neurally mediated cholinergic responses contributed to the inhibitory effect on propulsive activity. H_2S effects were not related to changes in the frequency of slow wave activity originating in the network of interstitial cells of Cajal located near the submuscular plexus. Luminal H_2S did not modify colonic motility probably because of epithelial detoxification.

Abbreviations
CBS, cystathionine β-synthase; CSE, cystathionine γ-lyase; EFS, electrical field stimulation; EJP, excitatory junction potential; ICC, interstitial cells of Cajal; ICC-SMP, ICC associated with the submuscular plexus; ICC-MP, ICC associated with the myenteric plexus; IJP, inhibitory junction potential; K_{ATP}, ATP-sensitive potassium channels; L-NNA, N^{ω}-nitro-L-arginine; MRS2500, (1R,2S,4S,5S)-4-[2-iodo-6-(methylamino)-9H-purin-9-yl]-2-(phosphonooxy)bicyclo [3.1.0]hexane-1-methanol dihydrogen phosphate ester diammonium salt; ODQ, 1H-[1,2,4]oxadiazolo[4,3-α]quinoxalin-1-one; RPMCs, rhythmic propulsive motor complexes; RMP, resting membrane potential; SK_{Ca}, small conductance calcium-activated potassium channels; S-T maps, spatio-temporal maps; TTX, tetrodotoxin

Introduction

Gasotransmitters are gas molecules endogenously synthesized in a regulated manner, causing well-defined physiological and/or pathophysiological effects, acting at specific cellular and molecular targets and employing specific mechanism(s) of inactivation (Wang, 2002; Li and Moore, 2007; Linden *et al.*, 2010). Hydrogen sulphide (H_2S) fulfils, at least in part, the criteria to be considered as an endogenous gaseous signalling molecule in the gastrointestinal tract with putative functions regulating motility (Jimenez, 2010; Linden *et al.*, 2010).

Endogenous production of H_2S in the gastrointestinal tract has been demonstrated in tissue homogenates (Hosoki *et al.*, 1997; Martin *et al.*, 2010) and colonic strips (Linden *et al.*, 2008; Gil *et al.*, 2011). Two pyridoxal-dependent enzymes, cystathionine β-synthase (CBS, EC 4.2.1.22) and cystathionine γ-lyase (CSE, EC 4.4.1.1), are mainly responsible for H_2S synthesis. A third route of H_2S synthesis involves 3-mercaptopyruvate sulphurtransferase in combination with cysteine aminotransferase (Shibuya *et al.*, 2009a,b). CBS and CSE have been found along the entire gastrointestinal tract (Martin *et al.*, 2010). Both enzymes are detected in several cell types including smooth muscle cells, enteric neurons, interstitial cells of Cajal (ICC) and epithelial cells, varying between species and regions of the gastrointestinal tract and suggesting that several cell types have the capacity to produce H_2S (Schicho *et al.*, 2006; Linden *et al.*, 2008; Hennig and Diener, 2009; Martin *et al.*, 2010; Gil *et al.*, 2011). Sulphide quinone reductase is responsible for H_2S catabolism in the muscularis externa of the colon and might be the main enzyme involved in the termination of H_2S-mediated signals (Linden *et al.*, 2012).

In the large intestine, luminal bacteria also represent a source of H_2S (Blachier *et al.*, 2010). However, although high concentrations of H_2S are present in the colon (mM range), the vast majority of H_2S is bound to luminal content (Jorgensen and Mortensen, 2001; Levitt *et al.*, 2002). Thus, low levels of free H_2S are available in the colonic lumen, being quickly metabolized in the colonic mucosa (Furne *et al.*, 2001; Blachier *et al.*, 2010).

Sodium hydrosulphide (NaHS) is commonly used as a source of H_2S in '*in vitro*' experiments. In the gastrointestinal tract, both excitatory and inhibitory effects on smooth muscle have been reported. For example, in the guinea pig and mouse stomach, H_2S causes dual effect, that is, a contraction is observed at low concentrations whereas at high concentrations H_2S causes relaxation (Zhao *et al.*, 2009; Han *et al.*, 2011). NaHS concentration-dependently relaxed prostaglandin $F_{2\alpha}$-contracted circular muscle strips of mouse fundus and distal colon (Dhaese and Lefebvre, 2009; Dhaese *et al.*, 2010). NaHS also exerted relaxant effects on guinea pig, rabbit and rat ileum and jejunum preparations (Hosoki *et al.*, 1997; Teague *et al.*, 2002; Nagao *et al.*, 2011; 2012; Kasparek *et al.*, 2012). Furthermore, NaHS inhibits peristaltic activity in the mouse small intestine and colon (Gallego *et al.*, 2008). Spontaneous circular smooth muscle contractions observed in rat and human colonic strips are also concentration-dependently inhibited by NaHS (Gallego *et al.*, 2008). However, the mechanisms underlying these relaxant effects are unclear and might include activation of myosin light chain phosphatase (Dhaese and Lefebvre, 2009; Nagao *et al.*, 2012), ATP-sensitive potassium channels (K_{ATP}) (Gallego *et al.*, 2008; Zhao *et al.*, 2009; Nagao *et al.*, 2012), small conductance calcium-activated potassium channels (SK_{Ca}) (Gallego *et al.*, 2008) and even sodium channel activation (Strege *et al.*, 2011; channel nomenclature follows Alexander *et al.*, 2011.). In addition, a direct effect on ICC, responsible for pacemaker activity, has also been reported (Parajuli *et al.*, 2010). All these data suggest that the potential mechanisms underlying motility changes are variable, which is consistent with the various effects of NaHS on different targets.

In the colon, different motor patterns cause propulsion and/or mixing of luminal contents, allowing absorption of water and electrolytes, storage of food residues and defecation. In a recent study, video recording of rat colonic motility and construction of spatio-temporal maps (S-T maps) have revealed two main motor patterns: (i) rhythmic propulsive motor complexes (RPMCs) and (ii) rhythmic propagating ripples (Huizinga *et al.*, 2011). The first pattern is characterized by large, propulsive contractions, propagating aborally at low frequency (1.2 cpm in the proximal colon and 0.5 cpm in the mid colon). The second one showed a higher frequency (about 10 cpm) with smaller amplitude contractions propagating both orally and aborally in the proximal colon (Huizinga *et al.*, 2011). Similar motility patterns have been described in experiments using strain-gauge transducers (Li *et al.*, 2002). It has been hypothesized that these patterns depend on both neural modulation and ICC-mediated pacemaker activity (Huizinga *et al.*, 2011). *In vitro*, electrophysiological experiments in rat colon have revealed that ICC associated with the submuscular plexus (ICC-SMP) mediate slow wave activity, which is related to high frequency contractions, whereas ICC associated with the myenteric plexus (ICC-MP) underlie cyclic depolarizations, related to low frequencycontractions (Pluja *et al.*, 2001).

In the present study, we characterized the effects of H_2S on motility patterns in colon segments and on muscle contractions in muscle strips and investigated a possible effect on pacemaker activity in the rat colon. Briefly, H_2S modulated colonic motility reducing RPMCs and enhancing the amplitude of ripples without modifying slow wave activity. Mechanisms involved in H_2S-induced relaxant effects included both hyperpolarization of smooth muscle cells caused by potassium channel activation and reduction of cholinergic excitatory neuromuscular transmission. It is important to characterize H_2S effects on motility for its therapeutic potential in the treatment of colonic inflammation (Fiorucci *et al.*, 2007; Wallace *et al.*, 2009).

Methods

Animals

All animal care and experimental procedures complied with and were approved by the local Animal Ethics Boards. All studies involving animals are reported in accordance with the ARRIVE guidelines for reporting experiments involving animals (Kilkenny *et al.*, 2010; McGrath *et al.*, 2010). A total of 60 animals were used in the experiments described here. Male Sprague-Dawley rats (8–10 weeks old, 300–350 g) were purchased from Charles River (Lyon, France for experiments

performed in Spain, and Saint Constant, QC, Canada for experiments carried out in Canada). Both in Spain and in Canada, animals were housed under controlled conditions: temperature 22°C ± 2°C, humidity 55% ± 10%, 12:12 h light–dark cycle and access to water and food *ad libitum*. For motility studies in colonic segments, animals were anaesthetized using isoflurane and killed by cervical dislocation (procedure approved by the McMaster's Animal Research Ethics Board, McMaster University, Hamilton, ON, Canada). For microelectrodes and organ bath experiments, animals were stunned and killed by decapitation and exsanguination 2–3 s afterward (procedure approved by the Ethics Committee of the Universitat Autònoma de Barcelona, Bellaterra, Spain).

Tissue samples

After opening the abdominal cavity, the colon was removed and placed in carbogenated (95% O_2 and 5% CO_2), ice-cold physiological saline solution. Colonic segments for motility studies of about 10–12 cm in length were prepared by flushing out the content with physiological saline solution. For electrophysiological and mechanical studies carried out in muscle strips, the colon was opened along the mesenteric border and pinned to a Sylgard® base (Dow Corning Corporation, Midland, MI, USA) (mucosa side up). The proximal and the mid colon were identified accordingly to anatomical criteria previously described (Alberti *et al*., 2005). Three different types of samples were prepared: (i) whole colon preparations to evaluate motor patterns in organ baths; (ii) samples prepared by peeling off the mucosal layer for electrophysiological studies to evaluate slow wave activity; and (iii) preparations removing both the mucosal and submucosal layers for electrophysiological studies to evaluate the membrane potential and the inhibitory and excitatory neuromuscular transmission. Circular muscle strips were cut 1 cm long and 0.3 cm wide.

Motility studies performed in colonic segments

Colonic segments were placed into an organ bath containing warmed carbogenated physiological saline solution (37 ± 1°C). Both the proximal and distal ends were cannulated and fixed to the bottom of the organ bath to prevent shortening of the preparation. The samples were perfused with physiological saline solution keeping the inflow pressure at 6 cm H_2O. The outflow was measured using a COBE pressure transducer (Sorin Biomedical Inc., Irvine, CA, USA) placed at the bottom of a collecting container (1 cm diameter). Then, the signal was amplified using a Grass LP 122 amplifier (Astro-Med, Brossard, QC, Canada) and was digitized using a MiniDigi 1A A-D converter and Axoscope 9 software (Pclamp 9 software, Molecular Devices, Toronto, ON, Canada). After a period of 30 min of equilibration, colonic segments showed spontaneous mechanical activity. Motility was recorded using a Sony HDR-SR11 Digital HD Video Camera (Sony Corporation, Tokyo, Japan) placed above the preparation. Using 7 min duration (25 frames s^{-1}) video recordings, S-T maps were calculated with an ImageJ plug in (Gut trace) with a Java algorithm loosely based on Hennig *et al*. (1999). The edges of the colon were identified, and the diameter of the colon was calculated for every pixel along the preparation and for each video frame. S-T maps were obtained by plotting the diameter of the colon as image intensity in greyscale over time (X-axis) for the whole length of the colon (Y-axis). Thus, the reduction of the diameter of the colon (contraction) was showed in black colour, whereas the increase in diameter (relaxation) was depicted in white. A proportional level of grey was associated to intermediate diameters. Pixels were calibrated using a metric scale ruler, and lengths and diameters were expressed in centimetres (cm). Time-plots were prepared by representing the changes in diameter over time at a particular point of the colon. In these plots, the X-axis (diameter) was inverted and, therefore, a reduction of the diameter (contraction) was observed as a positive inflexion whereas an increase of the diameter (relaxation) was plotted as a negative inflexion. Thus, the recordings obtained were oriented similarly to those obtained with muscle bath experiments. For the motility patterns observed, the frequency (contractions per minute – cpm), the amplitude (cm) and the duration (s) were measured using Clampfit software (Pclamp 9 software, Molecular Devices). The velocity of propagation (cm min^{-1}.) was measured using ImageJ software. The outflow was expressed as cm H_2O (pressure).

Intracellular microelectrode recording

Samples were pinned with the submucosal or circular muscle layer facing upward in a Sylgard-coated chamber, continuously perfused with carbogenated physiological saline solution at 37°C ± 1°C. Tissue was allowed to equilibrate for 1 h before starting the experiment. Circular smooth muscle cells were impaled with glass microelectrodes filled with 3 M KCl (30–60 MΩ of resistance). Membrane potential was measured by using standard electrometer Duo773 (WPI Inc., Sarasota, FL, USA). Tracings were displayed on an oscilloscope 4026 (Racal-Dana Ltd, Windsor, England) and simultaneously digitalized (100 Hz) with PowerLab 4/30 system and Chart 5 software for Windows (both from ADInstruments, Castle Hill, NSW, Australia). Experiments were performed in the presence of nifedipine (1 μM) to stabilize impalements. Inhibitory junction potentials (IJP) were elicited by electrical field stimulation (EFS) using single pulses (0.3 ms duration) and increasing amplitude voltage (8, 12, 16, 20, 24, 28, 32, 36 and 40 V). Excitatory junction potentials (EJP) were evaluated using the same stimulation parameters in the presence of L-NNA (1 mM) and MRS2500 (1 μM) to block nitrergic and purinergic neuromuscular transmission respectively. The amplitude (mV) and duration (s) of the EFS-induced IJP and EJP were measured before and after drug infusion. In samples in which submucosal layer was removed, resting membrane potential (RMP), expressed in mV, was estimated as the most probable bin of the frequency distribution of the membrane potential (0.1 mV bins; 30–60 s recordings) (Gil *et al*., 2010). Slow waves were recorded in samples including the submucosal layer and their frequency (cycles per minute – cpm), amplitude (mV) and duration (s) measured. In these samples, RMP was established as the average of the membrane potential between each slow wave (in mV).

Muscle bath studies

Strips (1 × 0.3 cm) including all colon layers were mounted in a 10 mL organ bath containing carbogenated physiological saline solution maintained at 37 ± 1°C. Contractions from the circular muscle layer were measured using an isometric force transducer (Harvard VF-1 Harvard Apparatus Inc., Holliston, MA, USA) connected to a computer through an ampli-

fier. Data were digitized (25 Hz) using Data 2001 software (Panlab, Barcelona, Spain) coupled to an A/D converter installed in the computer. A tension of 1 g was applied and tissues were allowed to equilibrate for 1 h after which strips displayed spontaneous phasic activity. The frequency (cpm), the amplitude (g) and the duration (s) of contractions were measured to estimate the mechanical activity.

Data analysis and statistics

Data are expressed as mean ± SEM. Differences in the motility (in colonic segments and strips), RMP and slow waves induced by a single addition of NaHS (1 mM) were compared using a paired Student's *t*-test. Motility patterns in colonic segments observed in the proximal and the mid colon and the effect observed with lidocaine and lidocaine + carbachol on motility patterns were compared using a paired Student's *t*-test as well. An unpaired Student's *t*-test was used to compare the hyperpolarizations caused by NaHS (1 mM) in samples including or devoid of the submucosal layer. One-way ANOVA followed by Bonferroni's multiple comparison test was used to evaluate the effect of serosal addition of NaHS (0.3 and 1 mM) on motility patterns observed in colonic segments and to compare the hyperpolarizations caused by NaHS (0.3 mM) in the presence of ODQ and potassium channel inhibitors to control values. The differences between the amplitude and duration of the EJP before and after NaHS infusion and the effect of L-NNA and ODQ on NaHS concentration response curves were compared by two-way ANOVA followed by Bonferroni's multiple comparison test. IC_{50} values were calculated using a conventional sigmoid concentration–response curve with variable slope. $P < 0.05$ was considered to indicate statistical significance. '*n*' values indicate the number of animals. Statistical analysis and curve fitting were performed with GraphPad Prism version 4.00, (GraphPad Software, San Diego, CA, USA).

Materials

The composition of the physiological saline solution was (in mM) glucose 10.10, NaCl 115.48, $NaHCO_3$ 21.90, KCl 4.61, NaH_2PO4 1.14, $CaCl_2$ 2.50 and $MgSO_4$ 1.16 (pH 7.3–7.4). The following drugs were used: tetrodotoxin (TTX) (Latoxan, Valence, France); apamin, carbachol (carbamoylcholine chloride), charybdotoxin, glibenclamide, lidocaine, nifedipine, N^{ω}-nitro-L-arginine (L-NNA), 1H-[1,2,4]oxadiazolo[4,3-α] quinoxalin-1-one (ODQ), sodium hydrogen sulphide (NaHS) (Sigma Chemicals, St. Louis, MO, USA); (1R,2S,4S,5S)-4-[2-iodo-6-(methylamino)-9H-purin-9-yl]-2-(phosphonooxy) bicyclo[3.1.0]hexane-1-methanol dihydrogen phosphate ester diammonium salt (MRS2500), 1-[(2-chlorophenyl) diphenylmethyl]-1*H*-pyrazole (TRAM-34) (Tocris, Bristol, UK). Stock solutions were made by dissolving drugs in distilled water except for nifedipine, ODQ and TRAM-34, which were dissolved in 96% ethanol, and L-NNA, which was dissolved in physiological saline solution by sonication.

Results

Motility patterns in colonic S-T maps

As previously described, two different motor patterns were observed in S-T maps obtained from video recordings from colonic segments of the rat: RPMCs and rhythmic propagating ripples (Huizinga *et al.*, 2011). RPMCs were observed in the proximal colon at a frequency of 1.3 ± 0.1 cpm ($n = 16$; Figure 1) and about 40% of them propagated to the mid colon (0.5 ± 0.1 cpm; $n = 16$; Figure 1). The amplitude of the contraction was lower in the proximal (2.2 ± 0.2 mm) compared to the mid colon (3.8 ± 0.2 mm $P < 0.001$; $n = 16$; Figure 1). The duration was higher in the mid than in the

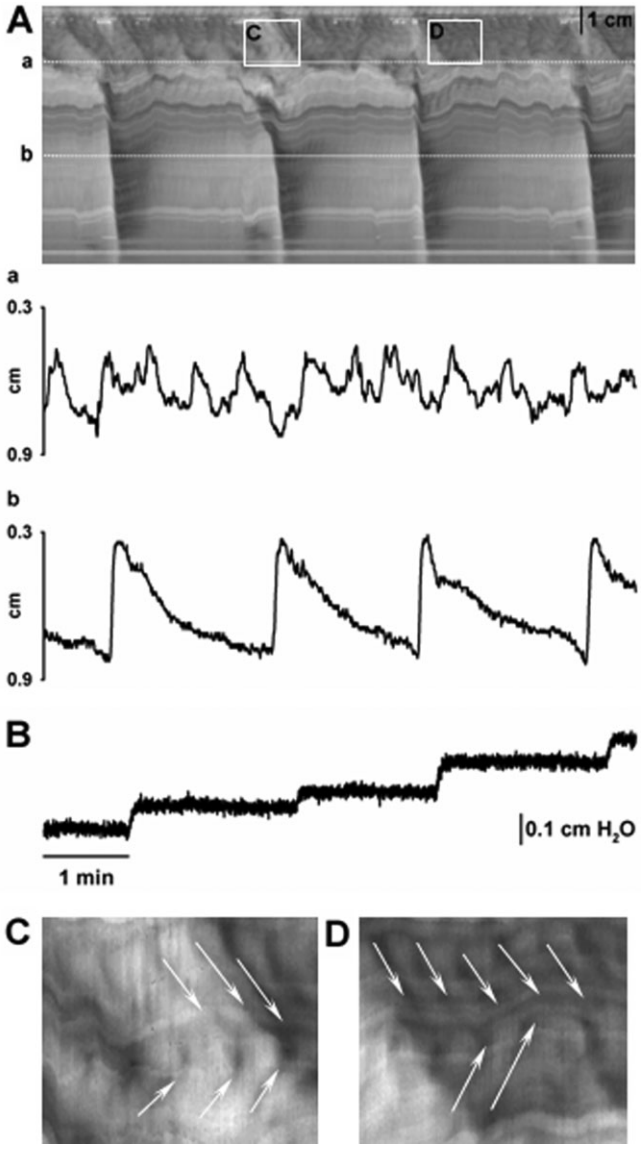

Figure 1

S-T map showing motor patterns observed in colonic segments (A). Note that black is narrowing of the lumen (contraction) and white is widening of the lumen (relaxation). RPMCs (large contractions) with superimposed ripples (small contractions) are observed in the proximal colon. RPMCs propagate aborally but only some of these contractions reached the mid colon. Detail of the diameter of the colon in the proximal (Aa) and mid (Ab) regions (dotted lines in S-T map). RPMCs in the mid colon are associated with outflow of content (B). Detail of ripples (arrows) observed in the proximal colon (C,D). Note that ripples propagate both orally and aborally.

Table 1

Effect of serosal and intraluminal addition of NaHS on RPMCs in the proximal and mid colon and ripples

		Serosal NaHS		Intraluminal NaHS	
RPMCs (proximal)	**Control**	**0.3 mM**	**1 mM**	**Control**	**1 mM**
Frequency (cpm)	1.4 ± 0.4	0.5 ± 0.3	0.0 ± 0.0[a]	1.1 ± 0.2	1.2 ± 0.2
Amplitude (mm)	2.0 ± 0.5	1.4 ± 0.5	0.0 ± 0.0[b]	1.9 ± 0.2	2.3 ± 0.5
Duration (s)	30.9 ± 4.9	35.1 ± 15.2	0.0 ± 0.0	37.9 ± 5.1	31.6 ± 5.1
Propagation (cm min^{-1})	5.8 ± 1.2	3.8 ± 1.3	0.0 ± 0.0[a]	5.2 ± 0.7	7.3 ± 2.5
RPMCs (mid)	**Control**	**0.3 mM**	**1 mM**	**Control**	**100 μM**
Frequency (cpm)	0.6 ± 0.1	0.1 ± 0.1[c]	0.0 ± 0.0[c]	0.5 ± 0.1	0.5 ± 0.1
Amplitude (mm)	3.0 ± 0.3	0.9 ± 0.9[a]	0.0 ± 0.0[b]	3.5 ± 0.6	3.4 ± 0.7
Duration (s)	60.9 ± 12.2	34.2 ± 34.2	0.0 ± 0.0	65.3 ± 8.9	66.1 ± 15.1
Propagation (cm min^{-1})	14.8 ± 9.2	0.2 ± 0.2	0.0 ± 0.0	11.6 ± 2.5	23.6 ± 6.0[a]
Ripples	**Control**	**0.3 mM**	**1 mM**	**Control**	**100 μM**
Frequency (cpm)	9.5 ± 0.5	9.2 ± 0.2	9.6 ± 0.4	9.6 ± 1.0	8.9 ± 0.3
Amplitude (mm)	0.4 ± 0.1	0.7 ± 0.1[a]	0.9 ± 0.1[c]	0.5 ± 0.1	0.6 ± 0.1
Duration (s)	4.6 ± 0.2	5.1 ± 0.4	5.9 ± 0.3	4.9 ± 0.5	5.4 ± 0.4
Presence (cm)*	3.5 ± 0.2	4.3 ± 0.6	6.4 ± 0.8[a]	3.5 ± 0.3	3.8 ± 0.6
Propagation (cm min^{-1})					
Aboral (anterograde)	6.8 ± 2.0	7.9 ± 1.6	7.0 ± 1.2	9.9 ± 2.6	6.6 ± 1.4
Oral (retrograde)	5.8 ± 0.8	5.5 ± 0.5	6.1 ± 0.8	7.5 ± 2.1	7.0 ± 1.1

Values are means ± SEM. For each experiment $n = 4$. [a]$P < 0.05$; [b]$P < 0.01$; [c]$P < 0.001$, significant difference from control; one-way ANOVA, followed by Bonferroni's multiple comparison test (for serosal NaHS experiment) and paired Student's *t*-test (for intraluminal NaHS experiment). *Distance in which ripples were observed from the proximal edge of the colon.

proximal colon (proximal: 34.2 ± 2.0 s vs. mid: 57.5 ± 5.1 s; $P < 0.001$; $n = 16$; Figure 1). In all cases, RPMCs propagated in aboral direction (velocity of propagation in proximal colon: 5.2 ± 0.3 cm min^{-1}; and in mid colon: 21.3 ± 3.5 cm min^{-1}; $P < 0.001$; $n = 16$; Figure 1) and were associated with outflow (Figure 1). In contrast, ripples were mainly observed in the proximal colon (they were present in the proximal 36 ± 2% of the total length of the colon used in the experiment; $n = 16$). They propagated both in oral and aboral direction at similar velocity (oral: 6.2 ± 0.6 cm min^{-1} vs. aboral: 7.3 ± 0.8 cm min^{-1}; n.s.; $n = 16$; Figure 1). This pattern was characterized by shallow contractions (amplitude: 0.5 ± 0.1 mm and duration: 4.8 ± 0.1 s; $n = 16$) measured at a frequency of 10.4 ± 0.1 cpm ($n = 16$). Ripples were not associated with outflow but were superimposed on RPMCs (Figure 1).

NaHS, administered at the serosal side, concentration-dependently inhibited RPMCs causing a complete cessation of this activity at 1 mM ($n = 4$; Table 1; Figure 2). In contrast, the amplitude of the ripples was enhanced but no changes in their frequency, duration or velocity of propagation were observed ($n = 4$; Table 1; Figure 2). Furthermore, ripples were recorded in the 70 ± 7% of the total length of the colon reaching 6.4 ± 0.8 cm from the proximal edge at 1 mM ($n = 4$; Table 1; Figure 2). In contrast, luminal administration of NaHS ($n = 4$; 1 mM; 30 min) did not modify motility patterns ($n = 4$; Table 1; Figure 3).

In order to distinguish between putative myogenic and neurogenic effects of hydrogen sulphide, NaHS was tested in the presence of the neuronal sodium channel blocker lidocaine. Lidocaine (100 μM) *per se* reduced RPMCs in the proximal colon and completely abolished RPMCs in the mid colon ($n = 4$; Table 2; Figure 4). In contrast, ripples were still recorded in the presence of lidocaine (100 μM) ($n = 4$; Table 2; Figure 4). In the presence of lidocaine (100 μM), NaHS abolished the remaining RPMCs in the proximal colon ($n = 4$; Figure 4) and concentration-dependently increased the amplitude of ripples ($n = 4$; Table 2; Figure 4).

As we previously described (Huizinga *et al.*, 2011), carbachol (10 μM) restored RPMCs after the blockade produced by lidocaine (100 μM) ($n = 4$; Table 3; Figure 4) showing that RPMCs were independent of neuronal cyclic activity but dependent on cholinergic neuronal input. Moreover, ripples were still recorded with characteristics similar to those observed in control ($n = 4$; Table 3; Figure 4). In the presence of lidocaine (100 μM) and carbachol (10 μM), NaHS caused effects similar to those observed in control conditions ($n = 4$; Table 3, Figure 4).

Mechanical activity in strips using muscle bath

Low frequency and high frequency contractions are observed in muscle bath recordings using isolated colonic strips with

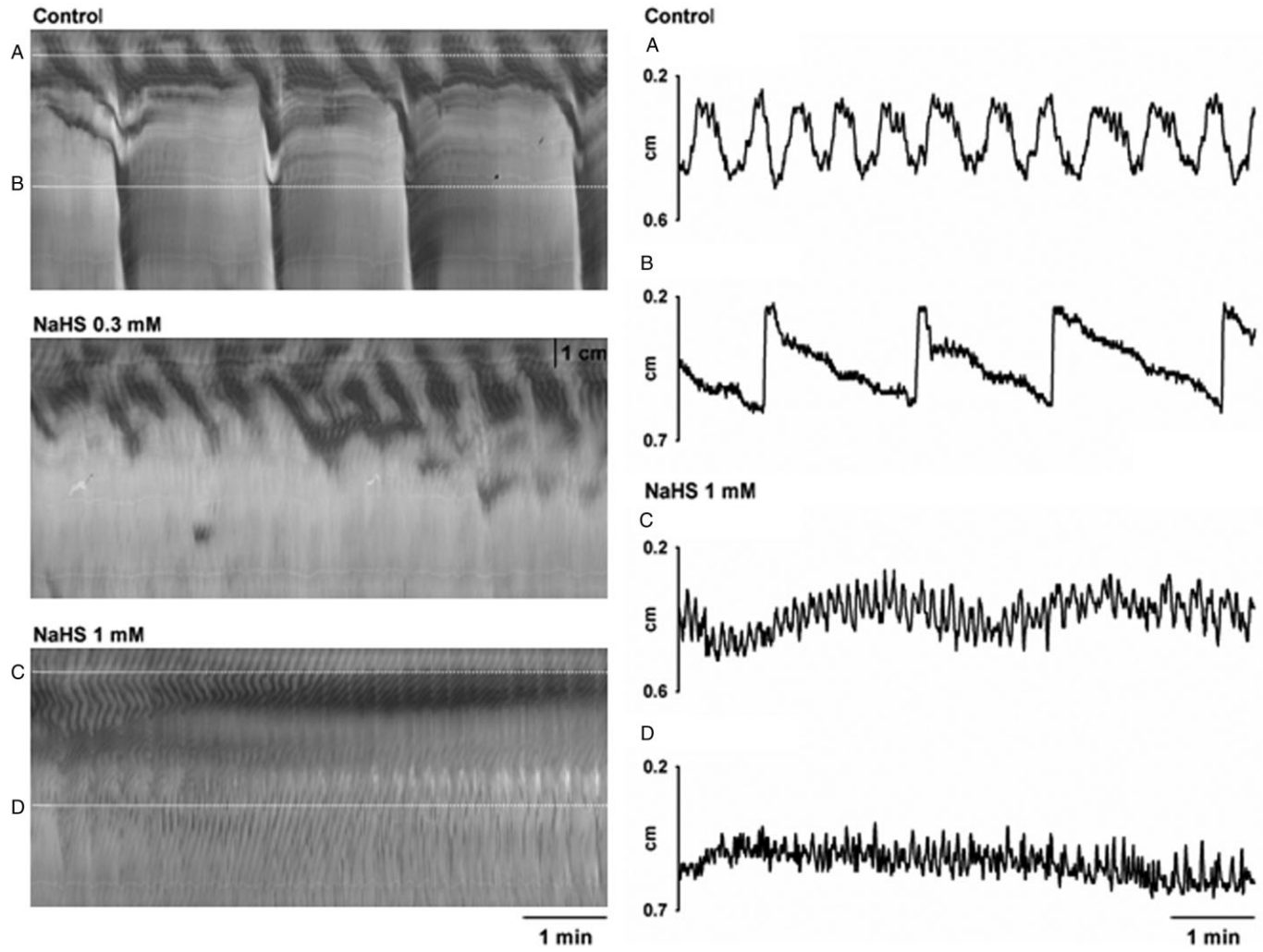

Figure 2

S-T maps (on the left) showing the effect produced by the serosal addition of NaHS (0.3 and 1 mM) on motor patterns observed in colonic segments. Detail of the diameter of the colon in the proximal (A) and mid (B) regions in control conditions and in the proximal (C) and mid (D) regions in the presence of NaHS (1 mM) (dotted lines in S-T maps). Note, on the right, that NaHS concentration-dependently inhibited RPMCs (large contractions) and increased the amplitude of ripples.

intact submucosal and myenteric plexuses (Pluja *et al.*, 2001; Alberti *et al.*, 2005). Both patterns are correlated with the activity observed in colonic segments; however, in isolated strips both activities were still recorded in the presence of TTX (1 μM). In mid colon strips, NaHS (1 mM) inhibited low frequency contractions, whereas high frequency contractions were still recorded (n = 4; Figure 5). It is important to note that the frequency of high frequency contractions was not modified by NaHS (n = 4; Figure 5). Furthermore, the amplitude of these contractions was not increased, as observed with ripples in colonic segments (n = 4; Figure 5). NaHS caused similar effects in the proximal colon and in the presence of the neuronal blocker TTX (1 μM) (data not shown).

RMP and slow wave activity

In order to properly evaluate the effect of NaHS on RMP, circular smooth muscle cells in strips devoid of the ICC network near the submuscular plexus (ICC-SMP), were impaled for electrophysiological recording. In this preparation, NaHS concentration-dependently hyperpolarized the smooth muscle cells (IC_{50} = 105.6 μM; log IC_{50} = –3.98 ± 0.33; n = 4; Figure 6A,B). ODQ (10 μM) slightly decreased NaHS (0.3 mM)-induced hyperpolarization. Glibenclamide (10 μM; n = 4), a K_{ATP} blocker, and apamin (1 μM; n = 4), a SK_{Ca} inhibitor, significantly reduced the effect of NaHS (0.3 mM) on smooth muscle membrane potential (Table 4; Figure 6C,D). A reduction of the NaHS (0.3 mM)-induced hyperpolarization was also observed when the tissue was pre-incubated with a cocktail of potassium channel blockers including apamin (1 μM), TRAM-34 (1 μM), glibenclamide (10 μM) and charybdotoxin (0.1 μM) (n = 3; Figure 6C,D).

To evaluate the effect of NaHS on slow wave activity, strips with an intact ICC-SMP network were studied. Slow waves were recorded in the presence of nifedipine (1 μM) at a frequency of 11.1 ± 0.8 cpm (n = 4; Figure 7). NaHS (1 mM) induced a smooth muscle hyperpolarization of –7.1 ± 1.8 mV

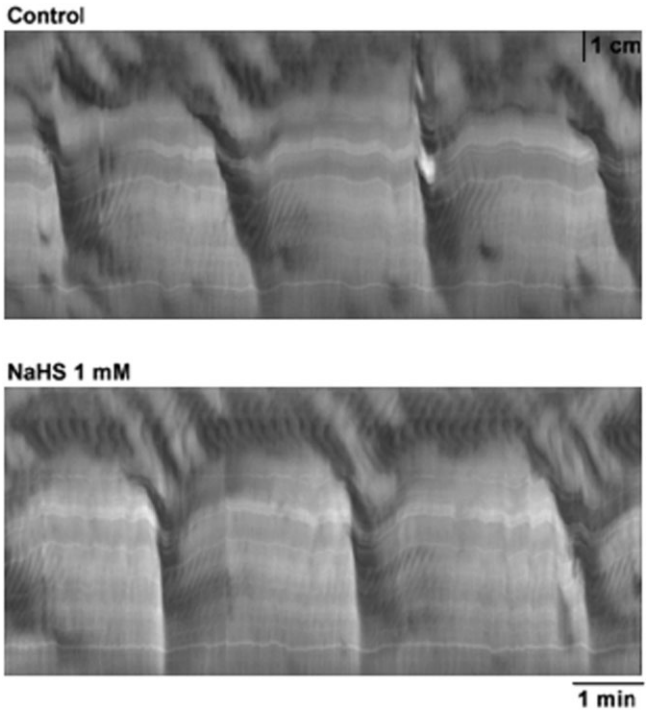

Figure 3

(A) S-T maps showing motor patterns observed in colonic segments under control conditions (top) and after the intraluminal addition of NaHS (1 mM) (bottom). No effect was observed.

($n = 4$; Figure 7A). Neither the frequency nor the duration nor the amplitude of slow waves was affected by NaHS (1 mM) infusion ($n = 4$; Figure 7B).

Interaction between NaHS, NO and guanylate cyclase (GC)

To evaluate a putative interaction between NaHS, NO and GC, rat colonic strips devoid of submucous plexus were studied. In the presence of TTX (1 μM), NaHS caused a concentration-dependent inhibition of mechanical activity (IC_{50} = 96.2 μM; log IC_{50} = –4.02 ± 0.04; $n = 9$; Figure 8A,B). Interestingly, when tissues were incubated with the GC inhibitor, ODQ (10 μM), the inhibitory effect of NaHS was reduced (IC_{50} = 252.5 μM; log IC_{50} = –3.60 ± 0.04; $P < 0.001$; $n = 7$; Figure 8A,B). However, in the presence of L-NNA (1 mM), NaHS was as potent an inhibitor as it was under control conditions (IC_{50} = 100.2 μM; log IC_{50} = –4.00 ± 0.05; n.s.; $n = 5$). Similar experiments had been previously performed with apamin and glibenclamide (Gallego *et al.*, 2008) and consequently were not repeated in the present study.

Effect of NaHS on neuromuscular transmission

Inhibitory neurotransmission was evaluated by measuring the amplitude and the duration of the IJP. None of these parameters was affected by NaHS (1 mM) (data not shown). In the presence of L-NNA (1 mM) and MRS2500 (1 μM), an atropine-sensitive EJP could be recorded (Figure 9A). The EJP amplitude was 3.0 ± 0.6 mV and the EJP duration was

Table 2

Effect of NaHS on RPMCs and ripples in the presence of lidocaine

		Lidocaine	Serosal NaHS	
RPMCs (proximal)	**Control**	**100 μM**	**0.3 mM**	**1 mM**
Frequency (cpm)	1.3 ± 0.3	0.5 ± 0.1[a]	0.0 ± 0.0[b]	0.0 ± 0.0[b]
Amplitude (mm)	2.0 ± 0.2	2.3 ± 0.4	0.0 ± 0.0[b]	0.0 ± 0.0[b]
Duration (s)	32.2 ± 3.3	21.7 ± 2.0	0.0 ± 0.0[c]	0.0 ± 0.0[c]
Propagation (cm min^{-1})	4.6 ± 0.2	5.8 ± 0.3[a]	0.0 ± 0.0[c]	0.0 ± 0.0[c]
		Lidocaine	**Serosal NaHS**	
Ripples	**Control**	**100 μM**	**0.3 mM**	**1 mM**
Frequency (cpm)	11.1 ± 0.9	13.4 ± 0.4	13.4 ± 0.9	11.1 ± 1.1[a]
Amplitude (mm)	0.6 ± 0.1	0.5 ± 0.1	0.8 ± 0.1	1.0 ± 0.2[a]
Duration (s)	4.7 ± 0.2	3.8 ± 0.2	4.4 ± 0.4	5.3 ± 0.7[a]
Presence (cm)*	3.5 ± 0.2	4.4 ± 0.6	5.9 ± 0.5	6.1 ± 0.9
Propagation (cm min^{-1})				
Aboral (anterograde)	6.3 ± 0.4	6.6 ± 1.0	5.6 ± 0.4	6.3 ± 0.4
Oral (retrograde)	6.0 ± 0.1	6.3 ± 0.2	6.3 ± 0.6	6.6 ± 0.9

Values are means ± SEM. $n = 4$. Note that lidocaine (100 μM) abolished RPMCs in the mid colon, therefore these data were not included in this table. [a]$P < 0.05$; [b]$P < 0.01$; [c]$P < 0.001$, significant difference from control or lidocaine (100 μM) respectively; paired Student's *t*-test (lidocaine vs. control) and one-way ANOVA, followed by Bonferroni's multiple comparison test (NaHS vs. lidocaine). *Distance in which ripples were observed from the proximal edge of the colon.

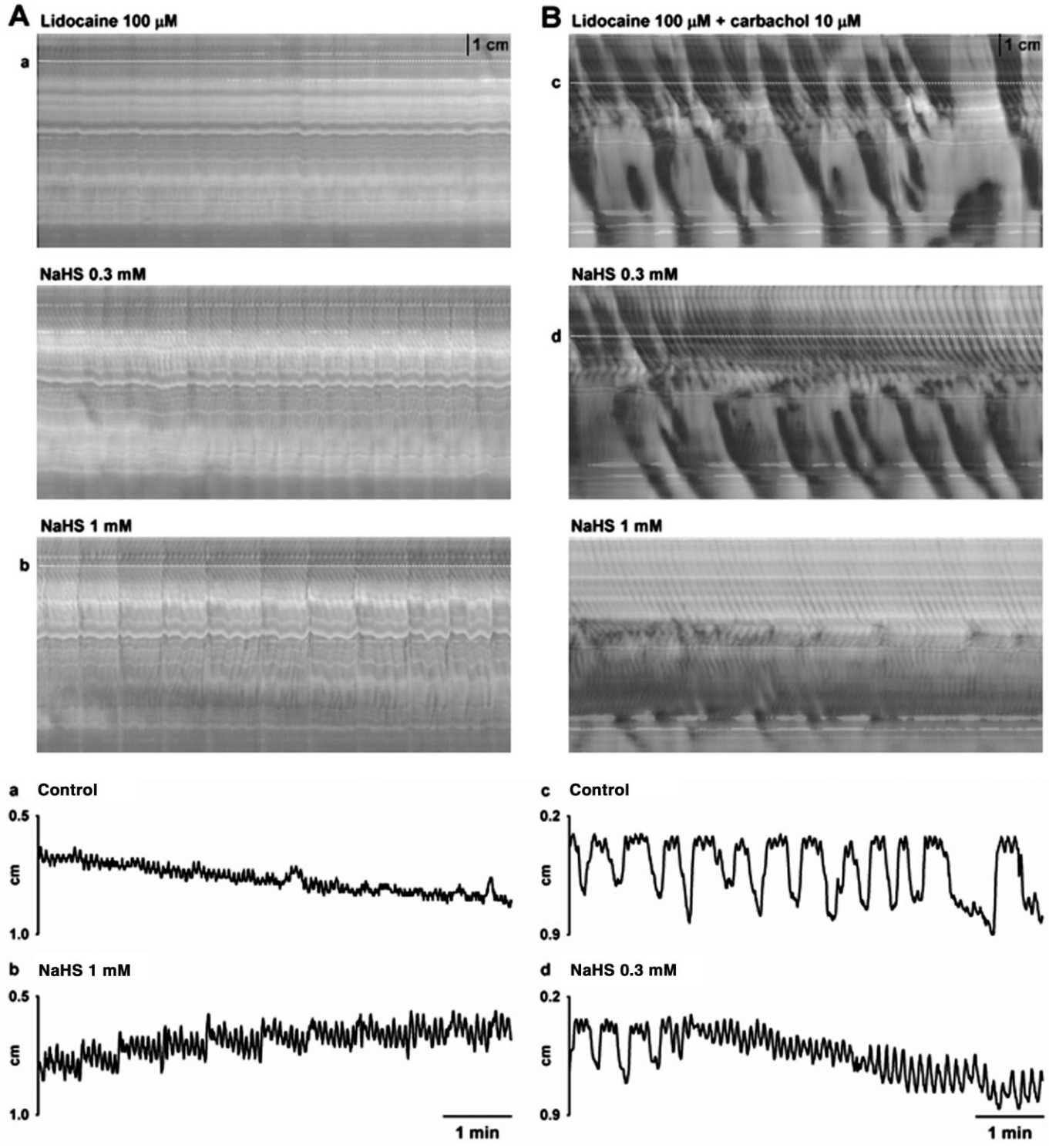

Figure 4

S-T maps showing the effect caused by the serosal addition of NaHS (0.3 and 1 mM) on motor patterns observed in colonic segments in the presence of lidocaine (100 μM) (A) and lidocaine (100 μM) + carbachol (10 μM) (B). Note that in the presence of lidocaine alone, ripples but not RPMCs are observed. Addition of carbachol restored RPMCs. Detail of the diameter of the colon in the proximal region in control conditions (Aa) and after the addition of NaHS (1 mM) (Ab) (dotted lines in S-T maps) in the presence of lidocaine (100 μM). Detail of the diameter of the colon in the proximal region in control conditions (Bc) and after the addition of NaHS (0.3 mM) (Bd) (dotted lines in S-T maps) in the presence of lidocaine (100 μM) + carbachol (10 μM). In both cases, NaHS caused effects similar to those observed in control conditions.

Table 3

Effect of NaHS on RPMCs and ripples in the presence of lidocaine and carbachol

RPMCs (proximal)	Control	Lidocaine (100 μM) + Carbachol (10 μM)	Serosal NaHS 0.3 mM	Serosal NaHS 1 mM
Frequency (cpm)	1.3 ± 0.1	1.8 ± 0.2[a]	0.0 ± 0.0[c]	0.0 ± 0.0[c]
Amplitude (mm)	2.9 ± 0.4	3.8 ± 0.2	0.0 ± 0.0[c]	0.0 ± 0.0[c]
Duration (s)	35.6 ± 2.6	26.3 ± 1.0[a]	0.0 ± 0.0[c]	0.0 ± 0.0[c]
Propagation (cm min^{-1})	5.2 ± 0.5	8.9 ± 1.0	0.0 ± 0.0[c]	0.0 ± 0.0[c]
RPMCs (mid)	**Control**	**Lidocaine (100 μM) + Carbachol (10 μM)**	**Serosal NaHS 0.3 mM**	**Serosal NaHS 1 mM**
Frequency (cpm)	0.8 ± 0.2	1.0 ± 0.2	0.8 ± 0.5	0.3 ± 0.3
Amplitude (mm)	4.2 ± 0.5	4.6 ± 0.6	2.2 ± 1.3[a]	0.1 ± 0.1[b]
Duration (s)	37.1 ± 8.8	29.9 ± 0.6	15.3 ± 9.4	6.2 ± 6.2
Propagation (cm min^{-1})	25.5 ± 4.0	10.4 ± 1.6	5.0 ± 3.2	3.6 ± 3.6[a]
Ripples	**Control**	**Lidocaine (100 μM) + Carbachol (10 μM)**	**Serosal NaHS 0.3 mM**	**Serosal NaHS 1 mM**
Frequency (cpm)	11.3 ± 0.2	10.1 ± 1.0	8.2 ± 0.4	9.5 ± 0.9
Amplitude (mm)	0.7 ± 0.1	0.8 ± 0.1	1.6 ± 0.1[a]	1.1 ± 0.4
Duration (s)	4.9 ± 0.1	4.9 ± 0.3	7.0 ± 0.3[b]	5.8 ± 0.6
Presence (cm)*	3.4 ± 0.4	5.4 ± 0.8	6.3 ± 0.8	7.3 ± 0.7
Propagation (cm min^{-1})				
Aboral (anterograde)	6.0 ± 0.5	6.5 ± 1.1	7.1 ± 0.8	7.1 ± 0.8
Oral (retrograde)	5.6 ± 0.7	7.8 ± 0.7[a]	7.2 ± 0.7	8.5 ± 1.5

Values are means ± SEM. $n = 4$. [a]$P < 0.05$; [b]$P < 0.01$; [c]$P < 0.001$, significant difference from control or lidocaine + carbachol respectively; paired Student's *t*-test (lidocaine + carbachol vs. control) and one-way ANOVA, followed by Bonferroni's multiple comparison test (NaHS vs. Lidocaine + carbachol). *Distance in which ripples were observed from the proximal edge of the colon.

Table 4

Effect of ODQ, glibenclamide, apamin and a combination of potassium channel blockers on smooth muscle membrane potential and hyperpolarization induced by NaHS

Treatment	*n*	Membrane potential (mV) Basal[1]	Pretreatment[2]	NaHS 0.3 mM[3]	Net effect on MP (mV) Pretreatment[2]	NaHS 0.3 mM[3]
Control	4	−40.8 ± 0.8	–	−50.3 ± 1.3[b]	–	−9.5 ± 0.8
ODQ 10 μM	4	−44.4 ± 2.2	−41.6 ± 2.8[a]	−48.3 ± 2.9[c]	+2.8 ± 0.7	−6.7 ± 0.5
Gliben 10 μM	4	−48.1 ± 2.0	−44.5 ± 2.9[a]	−48.7 ± 2.8[a]	+3.6 ± 1.1	−4.2 ± 0.7
Apamin 1 μM	4	−46.5 ± 3.1	−41.4 ± 2.4[a]	−45.2 ± 1.8[a]	+5.1 ± 1.2	−3.8 ± 0.7
K^+ blockers[4]	3	−40.0 ± 0.4	−36.4 ± 0.7	−39.2 ± 0.9	+3.6 ± 1.0	−2.8 ± 0.8

Values are means ± SEM. *n*, no. of samples. MP, membrane potential; Gliben, glibenclamide.
[1]Smooth muscle cells resting membrane potential (when no drug has been added).
[2]Pretreatment: effect of the drug (treatment column) incubated before NaHS.
[3]Effect of NaHS on smooth muscle membrane potential.
[4]Combination of K + blockers comprised glibenclamide 10 μM, apamin 1 μM, charybdotoxin 0.1 μM and TRAM-34 1 μM.
Note that positive and negative symbols included in the net effect column indicate the depolarization or the hyperpolarization observed by the drug (for pretreatment calculated from basal values and for NaHS 0.3 mM calculated from the values of membrane potential observed after the addition of the pretreatment drugs). [a]$P < 0.05$; [b]$P < 0.01$; [c]$P < 0.001$, significant differences; paired Student's *t*-test (pretreatment vs. basal and NaHS 0.3 mM vs. pretreatment; for control NaHS 0.3 mM was compared to basal).

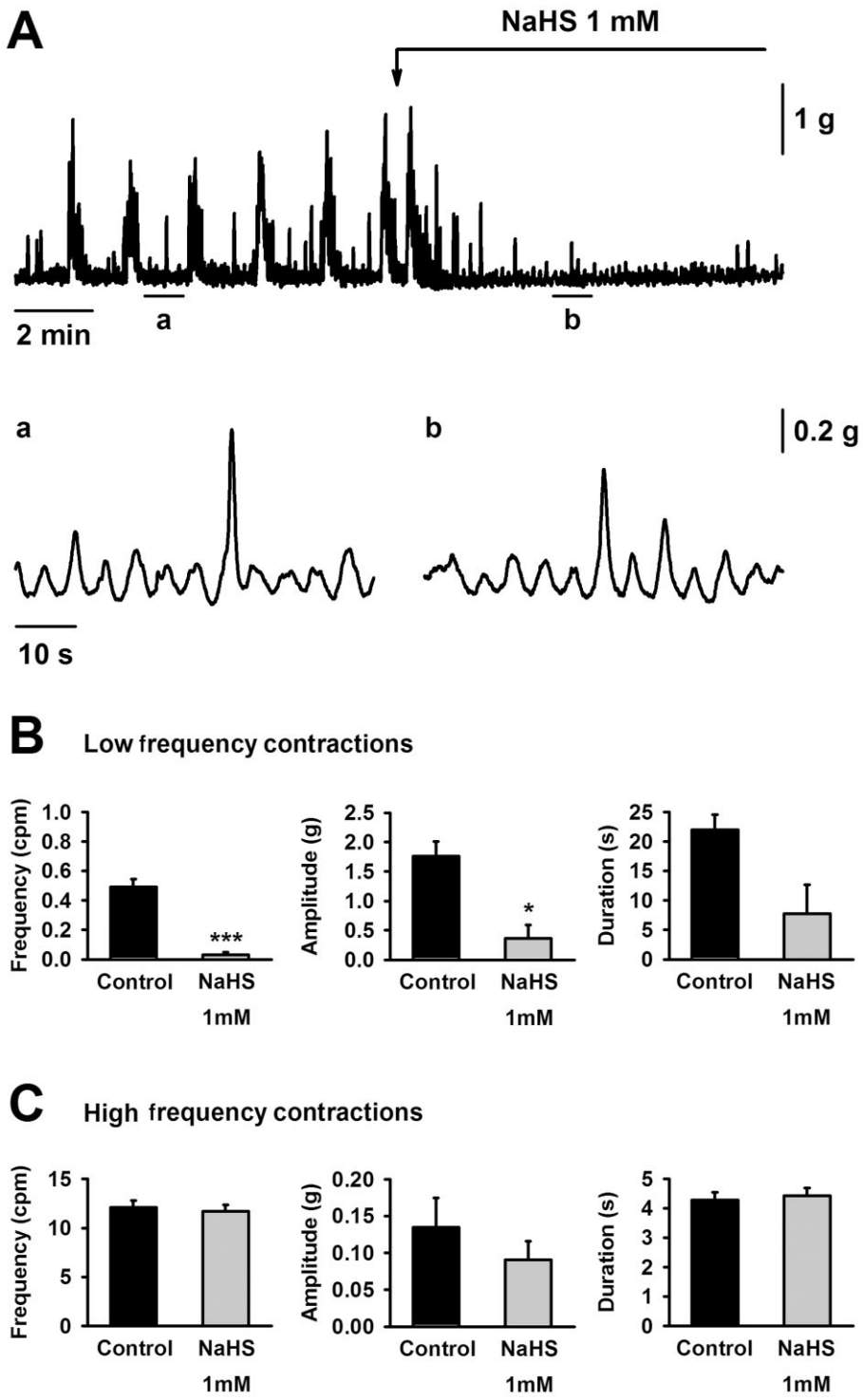

Figure 5

Muscle bath recordings showing the effect of NaHS (1 mM) on spontaneous mechanical activity in the rat mid colon (A). Detail of the high frequency contractions in control conditions (Aa) and in the presence of NaHS (1 mM) (Ab). Effect of NaHS (1 mM) on the frequency (left), amplitude (middle) and duration (right) of low frequency contractions (B) and high frequency contractions (C). All values are mean ± SEM. $n = 4$. *$P < 0.05$; ***$P < 0.001$, significant difference from control; paired Student's *t*-test.

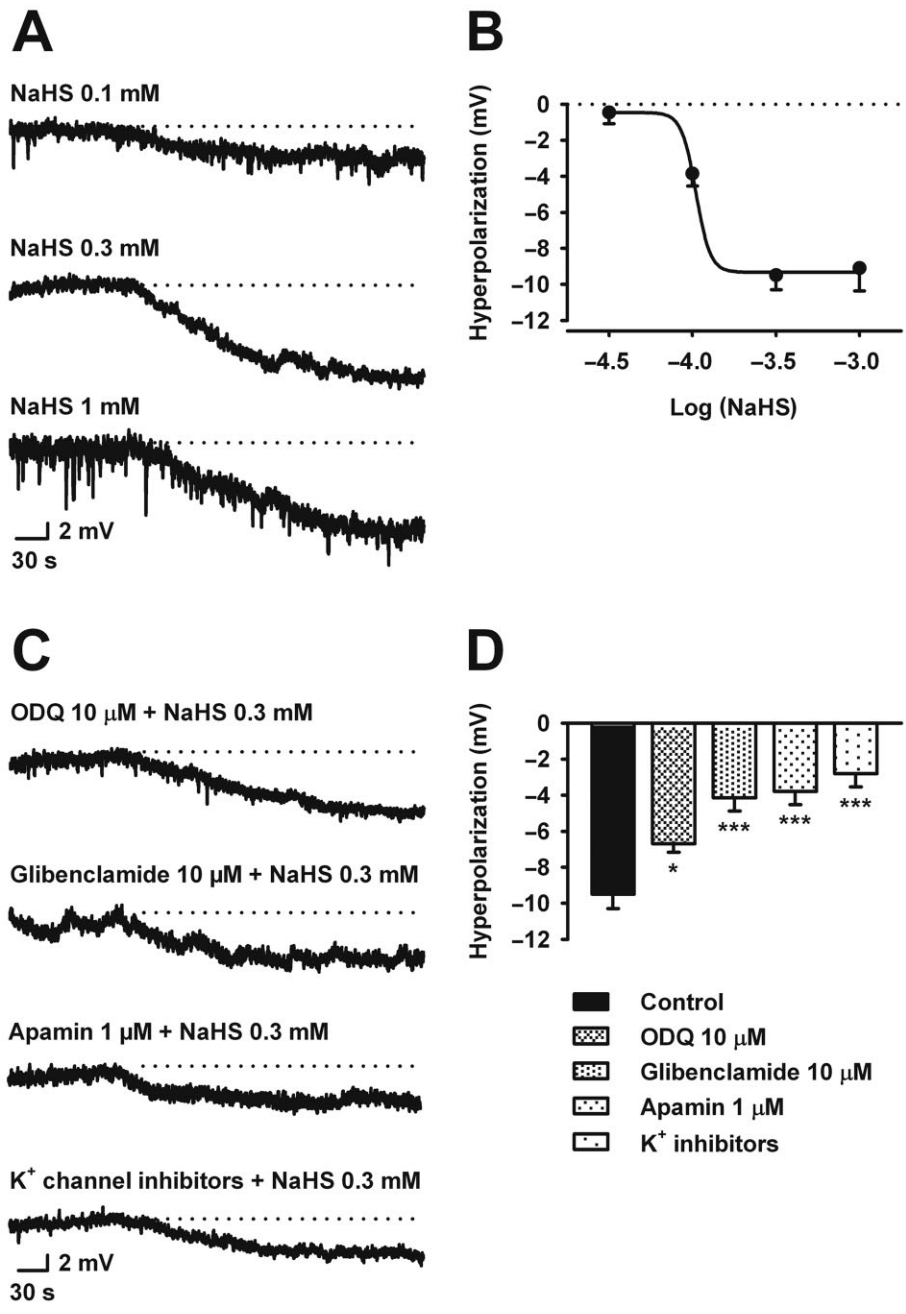

Figure 6

Intracellular microelectrode recordings showing the effect of NaHS (0.1 – 1 mM) on resting membrane potential in the rat mid colon (A). Dotted lines indicate the resting membrane potential. Concentration-response relationship for NaHS (B). Intracellular microelectrode recordings showing the hyperpolarization caused by NaHS (0.3 mM) in the presence of (i) ODQ (10 μM); (ii) glibenclamide (10 μM); (iii) apamin (1 μM); and (iv) a cocktail of potassium channel blockers including apamin (1 μM), TRAM-34 (1 μM), glibenclamide (10 μM) and charybdotoxin (0.1 μM) (from the top) (C). Dotted lines indicate the resting membrane potential. Histogram showing the effect of the different drugs mentioned above on the hyperpolarization produced by NaHS (0.3 mM) (D). All values are mean ± SEM. $n = 4$ for each experiment. *$P < 0.05$, ***$P < 0.001$, significant difference from control; one-way ANOVA, followed by Bonferroni's multiple comparison test.

1.3 ± 0.1 s at 32 V of stimulation ($n = 3$). The EJP was clearly inhibited by NaHS (1 mM) ($n = 3$; Figure 9B,C). In order to check that the effect was due to a pre- or post-junctional effect, the response to carbachol was tested in muscle bath experiments. To avoid post-junctional inhibitory effects due to smooth muscle hyperpolarization and consequently inhibition of L-type calcium channels, these experiments were performed in the presence of nifedipine. Under these conditions, carbachol induced a small atropine-sensitive contraction (Figure 9D), probably caused by calcium release from intracellular calcium stores (Oh *et al.*, 1997). The contractile responses induced by carbachol were decreased by NaHS

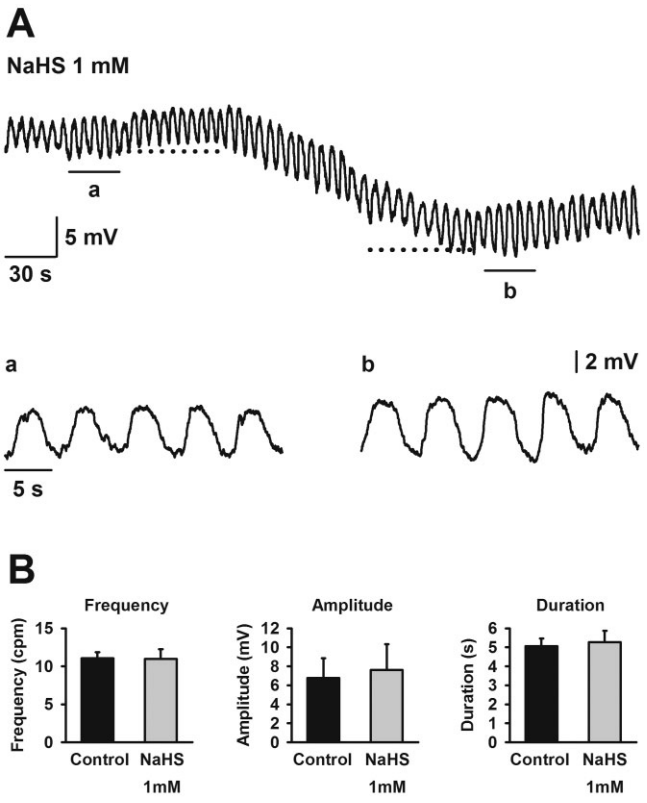

Figure 7

Intracellular microelectrode recordings showing slow waves recorded in samples with intact ICC-SMP network in the presence of nifedipine (1 μM) (A). Dotted lines indicate the resting membrane potential and the maximum hyperpolarization caused by NaHS (1 mM) respectively. Detail of slow waves in control conditions (Aa) and in the presence of NaHS (1 mM) (Ab). Histograms showing that NaHS (1 mM) did not modify frequency, amplitude or duration of slow waves (B). All values are mean ± SEM. $n = 4$. Significant differences were assessed using paired Student's *t*-test.

(1 mM) (carbachol 10 μM: 5.7 ± 0.8 g min^{-1} vs. carbachol 10 μM in the presence of NaHS 1 mM: 2.6 ± 0.2 g min^{-1} AUC; $P < 0.01$; $n = 5$; Figure 9D). Although we cannot completely rule out a pre-junctional effect, these experiments demonstrate that, at least in part, NaHS acted post-junctionally on cholinergic myogenic responses.

Discussion

In the present study, we investigated the effect of NaHS on colonic motor patterns in the rat colon. S-T maps of intestinal segments are an interesting methodology to characterize motility patterns *in vitro* and to study responses to different stimuli, that is, luminal distension or luminal and serosal drug application (Hennig *et al.*, 1999; 2010; D'Antona *et al.*, 2001; Berthoud *et al.*, 2002; Janssen *et al.*, 2007; Lentle *et al.*, 2007; 2008; Dinning *et al.*, 2012). Two motor patterns are identified in rat colonic S-T maps (Huizinga *et al.*, 2011 and present study). RPMCs were observed in the proximal colon

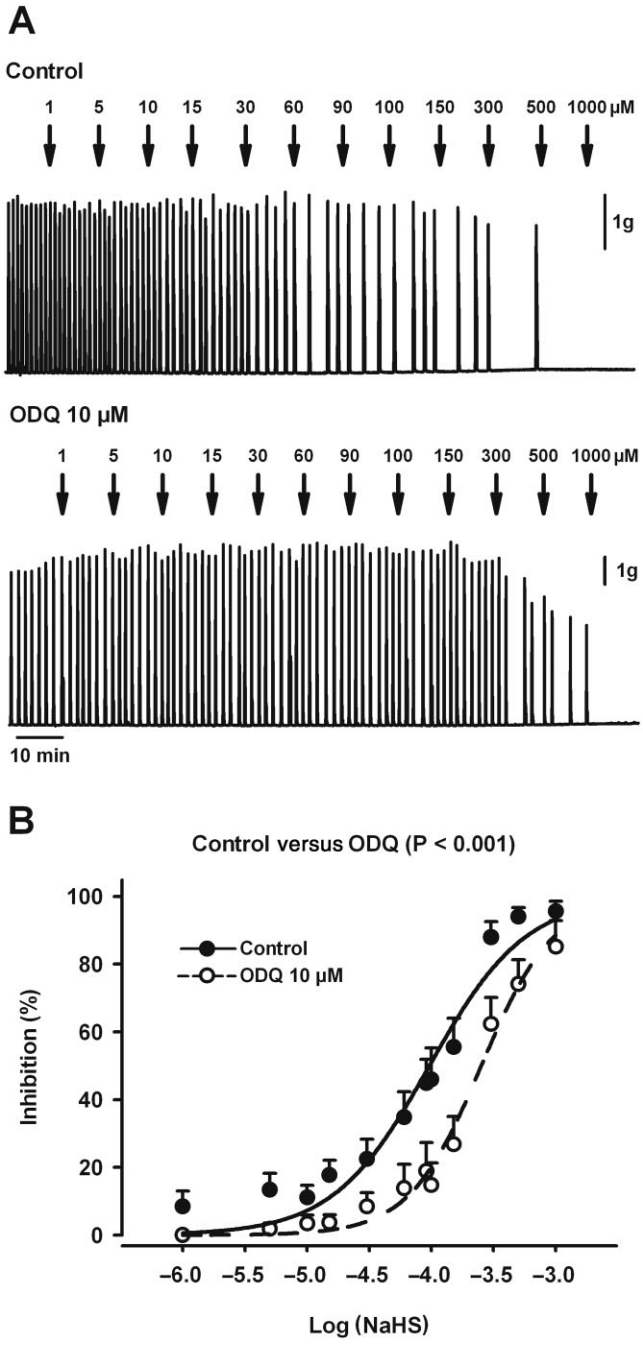

Figure 8

Effect of NaHS on spontaneous motility in muscle strips devoid of mucosa and submucosa. (A) Muscle bath recordings showing the concentration-dependent effect of NaHS (1–1000 μM) on spontaneous mechanical activity in the presence of TTX (1 μM) (upper recording) or TTX (1 μM) and ODQ (10 μM) (lower recording). (B) Concentration–response curves for NaHS in control conditions and in the presence of ODQ (10 μM). All values are mean ± SEM. Control, $n = 9$; ODQ, $n = 7$. Significant differences were assessed using two-way ANOVA, followed by Bonferroni's multiple comparison test.

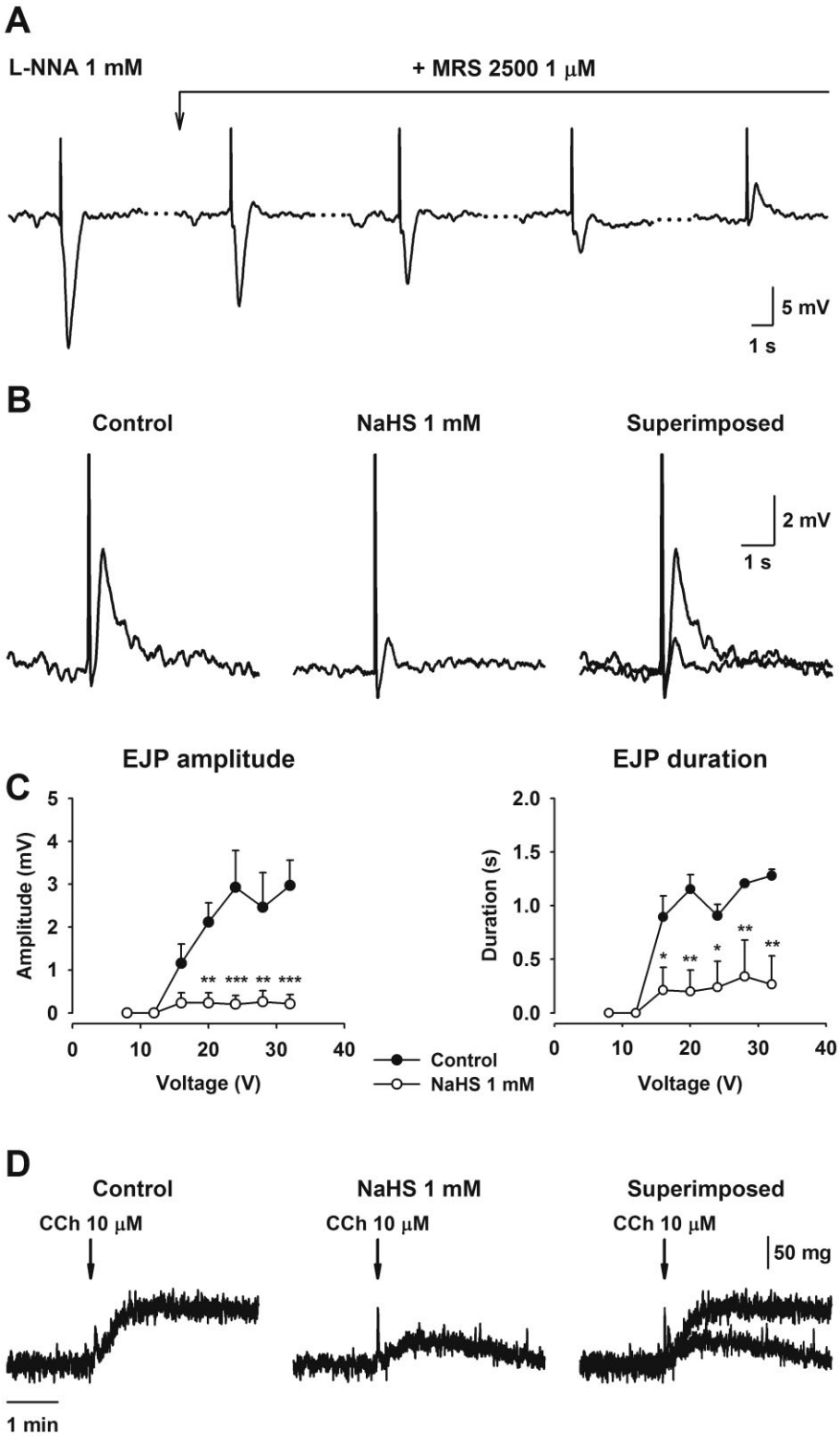

Figure 9

Intracellular microelectrode recordings showing how, in the presence of L-NNA (1 mM), MRS2500 (1 μM) gradually blocked the purinergic IJP revealing a hidden EJP (A). Breaks in the time axis are indicated by dotted lines. The EJP was clearly reduced by NaHS (1 mM) (B). The graphs represent the inhibitory effect of NaHS (1 mM) on both the amplitude and duration of the EFS-induced EJP (C). Muscle bath recordings in the presence of nifedipine (1 μM) showing the effect of NaHS 1 mM on contractile responses induced by carbachol (10 μM) (D). All values are mean ± SEM. Electrophysiological experiments: $n = 3$; muscle bath experiments: $n = 5$. *$P < 0.05$; **$P < 0.01$; ***$P < 0.001$, significant difference from control; two-way ANOVA, followed by Bonferroni's post test.

and about a quarter propagated to the mid colon causing a contraction strong enough to cause outflow. The second pattern consisted of high frequency, low-amplitude contractions, ripples, which propagated both in oral and aboral direction. Ripples did not cause outflow and hence were likely to promote mixing. Interestingly, similar motility patterns have been identified *in vivo* in rodents using other techniques such as strain-gauge transducers (Li *et al.*, 2002) or colonic manometry (Croci *et al.*, 1994). Therefore, construction of S-T maps is an interesting methodology to study motility in colonic segments *in vitro*. In the present work, we found that NaHS caused inhibition of RPMCs and enhancement of the amplitude of ripples without a major effect on their frequency and duration. Hence, ripples were the dominant pattern of motility both in the proximal and mid colon when tissue samples were incubated with NaHS. These results showed that NaHS inhibited propulsive movements in the colon and enhanced mixing movements. It is not known if the overall effect of NaHS will contribute to water absorption because both neuronally mediated and direct prosecretory effects of NaHS have been described in the colon (Schicho *et al.*, 2006; Hennig and Diener, 2009; Krueger *et al.*, 2010; Pouokam and Diener, 2011). Interestingly, changes in motility were observed when tissue was incubated with NaHS at the serosal side mimicking the location of H_2S as an endogenous mediator. In contrast, no effects were observed when NaHS was perfused in the lumen. This result is consistent with the marked capacity of colonic epithelial cells to metabolized H_2S (Furne *et al.*, 2001; Mimoun *et al.*, 2012). Thus, it is possible that H_2S produced by the microbiota does not reach the 'contractile' apparatus and, therefore, luminal H_2S is unlikely to modify mechanical activity, under physiological conditions. We can hypothesize that only when the intestinal barrier is disrupted (i.e. possibly when permeability is increased) or the inactivation by the epithelium is impaired, then luminal H_2S might reach, possibly by diffusion or via the blood stream, the zone where smooth muscle, neurons and ICC work cooperatively to organize motility.

Strips develop two types of myogenic contractions that we previously defined as low frequency (0.5–2 cpm) and high frequency contractions (10–12 cpm) (Alberti *et al.*, 2005). Using selective dissections (Pluja *et al.*, 2001) and animals with impaired ICC development (Alberti *et al.*, 2007), we have demonstrated that both ICC networks are necessary to record low frequency and high frequency contractions respectively. Both types of contractions are orchestrated by rhythmic oscillations in the RMP of smooth muscle cells: cyclic depolarizations with strong superimposed spiking activity, probably originating from the ICC associated with the myenteric plexus (ICC-MP), underlying low frequency contractions, and slow waves, likely to originate from the ICC associated with the submuscular plexus (ICC-SMP), causing high frequency contractions (Pluja *et al.*, 1999; 2001; Martin *et al.*, 2004; Alberti *et al.*, 2007). Although both experimental conditions are not identical (i.e. strips are stretched and the enteric circuitry is possibly partially disrupted), a correlation in terms of amplitude and frequency of contractions can be established between low frequency contractions recorded in the muscle bath and RPMCs observed in segments and between high frequency contractions and ripples (Pluja *et al.*, 2001; Alberti *et al.*, 2005; Huizinga *et al.*, 2011). Briefly: (i) the frequencies of high frequency contractions and ripples as well as low frequency contractions and RPMCs are similar; (ii) a gradient in frequency (higher in proximal colon) is observed in low frequency contractions, which is similar to the gradient in frequency observed in RPMCs; (iii) both high frequency contractions and ripples have a constant frequency all along the colon; (iv) low frequency contractions are usually of high amplitude, which is similar to the RPMCs, which aborally propagate and cause propulsion and outflow; and (v) the amplitude of high frequency contractions in strips is low, similar to that of ripples. Accordingly, similar motility patterns are observed both in strips and colonic segments despite the important differences in experimental conditions. In strips, NaHS inhibits low frequency contractions without modifying high frequency contractions (Gallego *et al.*, 2008 and present study). This suggests that in small strips the mechanism responsible for low frequency contractions is more sensitive to NaHS than the mechanism responsible for high frequency contractions, which is similar in segments and muscle strips. At the moment, we do not know why the amplitude of ripples is enhanced.

An important difference between segments and muscle strips is the sensitivity to neuronal blockade. In muscle bath recordings, low frequency and high frequency contractions are still observed in the presence of TTX showing that the musculature intrinsically has the mechanism to develop both patterns (Pluja *et al.*, 2001). In contrast, neuronal blockade selectively inhibits RPMCs without modifying the frequency of ripples [present paper and (Huizinga *et al.*, 2011)]. One conclusion might be that the enteric nervous system orchestrates both the pattern and the force of contraction. However this may not be the case because after neuronal blockade, carbachol can re-establish RPMCs and consequently this motility pattern does not depend on cyclic activation of motor neurons (neural pacemaker). Under the experimental conditions of the segment studies, the ICC-MP act as pacemaker cells with neuronal input essential for RPMCs (Huizinga *et al.*, 2011). Interestingly NaHS inhibited RPMCs and enhanced ripples after neuronal blockade and subsequent restoration of the motility with carbachol, suggesting that NaHS can also affect muscle activity through non-neuronal pathways.

In colon strips, the circular muscle layer is predominantly innervated by inhibitory motor neurons releasing nitric oxide and ATP (Grasa *et al.*, 2009; Gil *et al.*, 2010; 2012). In the present study, we used a combination of L-NNA and MRS2500 to block inhibitory neurotransmission. Under these conditions, atropine-sensitive EJPs were recorded. This particular experimental approach allowed us to evaluate the effect of NaHS on the excitatory neuromuscular transmission. Interestingly, NaHS inhibited cholinergic EJPs induced by EFS. In addition, NaHS also inhibited carbachol-mediated contractions in the presence of nifedipine. These experiments were performed in the presence of nifedipine to exclude the possibility that the effect observed with NaHS on carbachol-induced contractions was related to muscle hyperpolarization (see below). Therefore, inhibition of cholinergic neuromuscular transmission at the post-junctional level, is a possible mechanism that might explain the effect of NaHS on RPMCs, that is, NaHS inhibits cholinergic input mimicking the effect of atropine that also blocks RPMCs [present study and

(Huizinga *et al.*, 2011)]. Consistent with these results, it has been demonstrated that H_2S inhibited cholinergic contractions in the rabbit ileum (Teague *et al.*, 2002) and relaxed carbachol pre-contracted preparations of guinea pig taenia caecum (Denizalti *et al.*, 2011).

However, strips develop low frequency contractions even in the presence of atropine (i.e. classical NANC conditions). Consequently, inhibition of cholinergic responses cannot be responsible for the inhibitory effect observed in the muscle strips. Thus, our observed effect of smooth muscle hyperpolarization is a more likely mechanism. It is important to note that, as cyclic depolarizations are nifedipine-sensitive (Pluja *et al.*, 2001), a slight hyperpolarization (i.e. NaHS effect) might be enough to markedly reduce opening probability of L-type calcium channels and contractions will be consequently inhibited. The mechanism responsible for NaHS-induced hyperpolarization and inhibition of spontaneous low frequency contractions is probably quite complex and several mechanisms should be taken into account. The first possibility is that NaHS is causing NO release from inhibitory motor neurons leading smooth muscle hyperpolarization and relaxation. However, in the presence of L-NNA, NaHS caused similar inhibition of spontaneous motility and, therefore, the mechanism was independent of nNOS. Interestingly, ODQ partially inhibited both NaHS-induced hyperpolarization and inhibition of spontaneous motility suggesting that GC is a potential target for NaHS. Recently, it has been demonstrated that NaHS induced release of NO from nitrosothiols in rat brain homogenates (Ondrias *et al.*, 2008). Therefore, it might be possible that the inhibitory effects observed with NaHS were due to NO release from this type of NO donor with subsequent activation of GC (Gil *et al.*, 2012). Another potential mechanism is a direct or indirect effect on potassium channels, which would be consistent with our previous results obtained in muscle bath (Gallego *et al.*, 2008). The present study demonstrates that apamin and glibenclamide partially reduce the hyperpolarization induced by NaHS, confirming a potential role for SK_{Ca} and K_{ATP} channels mediating NaHS effects. However, it is important to note that the 'cocktail' of potassium channel inhibitors was more effective in reducing NaHS hyperpolarization, suggesting that the NaHS effects are unlikely to be mediated by a single potassium channel. Our results suggest that smooth muscle hyperpolarization might be the outcome of different direct and indirect mechanisms.

The question is then, does hyperpolarization affect the slow waves? Recordings in strips with the intact submucosa and ICC-SMP allow the measurement of slow wave activity that occurs at a similar frequency to high frequency contractions and ripples. Interestingly, NaHS causes a 7–8 mV hyperpolarization, which does not affect the frequency of the dominant slow wave driven pacemaker system, showing that slow wave activity, in terms of frequency, is independent of membrane potential (Ohba *et al.*, 1975; Jimenez *et al.*, 1999). Consistent with this finding, the frequency of slow waves was unaffected by long-lasting hyperpolarizations induced by endogenous inhibitory neurotransmitters released by EFS (unpublished data). This is consistent with different innervations of the two pacemaker systems.

We conclude that H_2S modulated colonic motility by inhibiting RPMCs and enhancing the amplitude of ripples, probably promoting mixing. Under physiological conditions, epithelial detoxification is probably able to limit the quantity of luminal H_2S that reaches the contractile apparatus and, therefore, no effects on motility are observed when NaHS is luminally applied. The mechanisms causing the effects on motility are diverse, which is consistent with the capacity of H_2S to affect different targets. In the present work, we demonstrated that cholinergic EJPs are inhibited, which is consistent with muscle bath experiments where the effect of NaHS on carbachol-induced contraction was measured. Inhibition of cholinergic neuronal responses might be consistent with the inhibition of RPMCs observed in S-T maps. However, *in vitro* low frequency contractions that were developed by intrinsic myogenic mechanisms are atropine insensitive. In this case, smooth muscle hyperpolarization might be crucial in the inhibition of these contractions. The frequency of slow waves was independent of cholinergic input and hyperpolarization caused by NaHS. Consequently, ripples, which are related to slow wave activity, were not inhibited by NaHS. Under our experimental conditions, H_2S shows relaxant properties and, therefore, further studies should be carried out to establish its putative use as an antispasmodic molecule (i.e. measurements of muscular tone and compliance), taking into account the potentiality of H_2S in the treatment of colonic inflammation (Fiorucci *et al.*, 2007; Wallace *et al.*, 2009).

Acknowledgements

The authors would like to thank Antonio Acosta and Claudia Arenas for their technical assistance. This work has been funded by the Ministerio de Ciencia e Innovación (Spain) and by the Agencia de Gestio d'Ajuts Universitaris de Catalunya (grant: 2011 CTP 00032). Work on spatio-temporal mapping was supported by an operating grant from the Canadian Institutes of Health Research to J. D. H., and V. G. was supported by the Ministerio de Ciencia e Innovación (Spain) (AP2007-01583). D. G. was supported by the Instituto de Salud Carlos III, Centro de Investigación Biomédica en red de enfermedades hepáticas y digestivas (CIBERehd).

Conflicts of interest

The authors state no conflict of interest.

References

Alberti E, Mikkelsen HB, Larsen JO, Jimenez M (2005). Motility patterns and distribution of interstitial cells of Cajal and nitrergic neurons in the proximal, mid- and distal-colon of the rat. Neurogastroenterol Motil 17: 133–147.

Alberti E, Mikkelsen HB, Wang XY, Diaz M, Larsen JO, Huizinga JD *et al.* (2007). Pacemaker activity and inhibitory neurotransmission in the colon of Ws/Ws mutant rats. Am J Physiol Gastrointest Liver Physiol 292: G1499–G1510.

Alexander SPH, Mathie A, Peters JA (2011). Guide to Receptors and Channels (GRAC), 5th edition (2011). Br J Pharmacol 164 (Suppl. 1): S1–S324.

Berthoud HR, Hennig G, Campbell M, Volaufova J, Costa M (2002). Video-based spatio-temporal maps for analysis of gastric motility in vitro: effects of vagal stimulation in guinea-pigs. Neurogastroenterol Motil 14: 677–688.

Blachier F, Davila AM, Mimoun S, Benetti PH, Atanasiu C, Andriamihaja M *et al*. (2010). Luminal sulfide and large intestine mucosa: friend or foe? Amino Acids 39: 335–347.

Croci T, Basilisco G, Bassani A, Manara L (1994). Manometric patterns of rat colonic motor activity and defecation. Effect of selective 5HT1A agonist 8-OH-DPAT. Dig Dis Sci 39: 1968–1973.

D'Antona G, Hennig GW, Costa M, Humphreys CM, Brookes SJ (2001). Analysis of motor patterns in the isolated guinea-pig large intestine by spatio-temporal maps. Neurogastroenterol Motil 13: 483–492.

Denizalti M, Durlu-Kandilci NT, Bozkurt TE, Sahin-Erdemli I (2011). Hydrogen sulphide inhibits carbachol-induced contractile responses in β-escin permeabilized guinea-pig taenia caecum. Eur J Pharmacol 658: 229–235.

Dhaese I, Lefebvre RA (2009). Myosin light chain phosphatase activation is involved in the hydrogen sulfide-induced relaxation in mouse gastric fundus. Eur J Pharmacol 606: 180–186.

Dhaese I, Van Colen I, Lefebvre RA (2010). Mechanisms of action of hydrogen sulfide in relaxation of mouse distal colonic smooth muscle. Eur J Pharmacol 628: 179–186.

Dinning PG, Costa M, Brookes SJ, Spencer NJ (2012). Neurogenic and myogenic motor patterns of rabbit proximal, mid, and distal colon. Am J Physiol Gastrointest Liver Physiol 303: G83–G92.

Fiorucci S, Orlandi S, Mencarelli A, Caliendo G, Santagada V, Distrutti E *et al*. (2007). Enhanced activity of a hydrogen sulphide-releasing derivative of mesalamine (ATB-429) in a mouse model of colitis. Br J Pharmacol 150: 996–1002.

Furne J, Springfield J, Koenig T, DeMaster E, Levitt MD (2001). Oxidation of hydrogen sulfide and methanethiol to thiosulfate by rat tissues: a specialized function of the colonic mucosa. Biochem Pharmacol 62: 255–259.

Gallego D, Clave P, Donovan J, Rahmati R, Grundy D, Jimenez M *et al*. (2008). The gaseous mediator, hydrogen sulphide, inhibits in vitro motor patterns in the human, rat and mouse colon and jejunum. Neurogastroenterol Motil 20: 1306–1316.

Gil V, Gallego D, Grasa L, Martin MT, Jimenez M (2010). Purinergic and nitrergic neuromuscular transmission mediates spontaneous neuronal activity in the rat colon. Am J Physiol Gastrointest Liver Physiol 299: G158–G169.

Gil V, Gallego D, Jimenez M (2011). Effects of inhibitors of hydrogen sulphide synthesis on rat colonic motility. Br J Pharmacol 164: 485–498.

Gil V, Gallego D, Moha Ou Maati H, Peyronnet R, Martinez-Cutillas M, Heurteaux C *et al*. (2012). Relative contribution of SKCa and TREK1 channels in purinergic and nitrergic neuromuscular transmission in the rat colon. Am J Physiol Gastrointest Liver Physiol 303: G412–G423.

Grasa L, Gil V, Gallego D, Martin MT, Jimenez M (2009). P2Y(1) receptors mediate inhibitory neuromuscular transmission in the rat colon. Br J Pharmacol 158: 1641–1652.

Han YF, Huang X, Guo X, Wu YS, Liu DH, Lu HL *et al*. (2011). Evidence that endogenous hydrogen sulfide exerts an excitatory effect on gastric motility in mice. Eur J Pharmacol 673: 85–95.

Hennig B, Diener M (2009). Actions of hydrogen sulphide on ion transport across rat distal colon. Br J Pharmacol 158: 1263–1275.

Hennig GW, Costa M, Chen BN, Brookes SJ (1999). Quantitative analysis of peristalsis in the guinea-pig small intestine using spatio-temporal maps. J Physiol 517 (Pt 2): 575–590.

Hennig GW, Gregory S, Brookes SJ, Costa M (2010). Non-peristaltic patterns of motor activity in the guinea-pig proximal colon. Neurogastroenterol Motil 22: e207–e217.

Hosoki R, Matsuki N, Kimura H (1997). The possible role of hydrogen sulfide as an endogenous smooth muscle relaxant in synergy with nitric oxide. Biochem Biophys Res Commun 237: 527–531.

Huizinga JD, Martz S, Gil V, Wang XY, Jimenez M, Parsons S (2011). Two independent networks of interstitial cells of Cajal work cooperatively with the enteric nervous system to create colonic motor patterns. Front Neurosci 5 (Art 93): 1–14.

Janssen PW, Lentle RG, Asvarujanon P, Chambers P, Stafford KJ, Hemar Y (2007). Characterization of flow and mixing regimes within the ileum of the brushtail possum using residence time distribution analysis with simultaneous spatio-temporal mapping. J Physiol 582 (Pt 3): 1239–1248.

Jimenez M (2010). Hydrogen sulfide as a signaling molecule in the enteric nervous system. Neurogastroenterol Motil 22: 1149–1153.

Jimenez M, Borderies JR, Vergara P, Wang Y, Daniel EE (1999). Slow waves in circular muscle of porcine ileum: structural and electrophysiological studies. Am J Physiol 276: G393–G406.

Jorgensen J, Mortensen PB (2001). Hydrogen sulfide and colonic epithelial metabolism: implications for ulcerative colitis. Dig Dis Sci 46: 1722–1732.

Kasparek MS, Linden DR, Farrugia G, Sarr MG (2012). Hydrogen sulfide modulates contractile function in rat jejunum. J Surg Res 175: 234–242.

Kilkenny C, Browne W, Cuthill IC, Emerson M, Altman DG (2010). NC3Rs Reporting Guidelines Working Group. Br J Pharmacol 160: 1577–1579.

Krueger D, Foerster M, Mueller K, Zeller F, Slotta-Huspenina J, Donovan J *et al*. (2010). Signaling mechanisms involved in the intestinal pro-secretory actions of hydrogen sulfide. Neurogastroenterol Motil 22: 1224–e320.

Lentle RG, Janssen PW, Asvarujanon P, Chambers P, Stafford KJ, Hemar Y (2007). High definition mapping of circular and longitudinal motility in the terminal ileum of the brushtail possum Trichosurus vulpecula with watery and viscous perfusates. J Comp Physiol B 177: 543–556.

Lentle RG, Janssen PW, Asvarujanon P, Chambers P, Stafford KJ, Hemar Y (2008). High-definition spatiotemporal mapping of contractile activity in the isolated proximal colon of the rabbit. J Comp Physiol B 178: 257–268.

Levitt MD, Springfield J, Furne J, Koenig T, Suarez FL (2002). Physiology of sulfide in the rat colon: use of bismuth to assess colonic sulfide production. J Appl Physiol 92: 1655–1660.

Li L, Moore PK (2007). An overview of the biological significance of endogenous gases: new roles for old molecules. Biochem Soc Trans 35: 1138–1141.

Li M, Johnson CP, Adams MB, Sarna SK (2002). Cholinergic and nitrergic regulation of in vivo giant migrating contractions in rat colon. Am J Physiol Gastrointest Liver Physiol 283: G544–G552.

Linden DR, Sha L, Mazzone A, Stoltz GJ, Bernard CE, Furne JK *et al*. (2008). Production of the gaseous signal molecule hydrogen sulfide in mouse tissues. J Neurochem 106: 1577–1585.

Linden DR, Levitt MD, Farrugia G, Szurszewski JH (2010). Endogenous production of H2S in the gastrointestinal tract: still in search of a physiologic function. Antioxid Redox Signal 12: 1135–1146.

Linden DR, Furne J, Stoltz GJ, Abdel-Rehim MS, Levitt MD, Szurszewski JH (2012). Sulphide quinone reductase contributes to hydrogen sulphide metabolism in murine peripheral tissues but not in the CNS. Br J Pharmacol 165: 2178–2190.

Martin MT, Hove-Madsen L, Jimenez M (2004). Otilonium bromide inhibits muscle contractions via L-type calcium channels in the rat colon. Neurogastroenterol Motil 16: 175–183.

Martin GR, McKnight GW, Dicay MS, Coffin CS, Ferraz JG, Wallace JL (2010). Hydrogen sulphide synthesis in the rat and mouse gastrointestinal tract. Dig Liver Dis 42: 103–109.

McGrath J, Drummond G, McLachlan E, Kilkenny C, Wainwright C (2010). Guidelines for reporting experiments involving animals: the ARRIVE guidelines. Br J Pharmacol 160: 1573–1576.

Mimoun S, Andriamihaja M, Chaumontet C, Atanasiu C, Benamouzig R, Blouin JM *et al*. (2012). Detoxification of H(2)S by differentiated colonic epithelial cells: implication of the sulphide oxidizing unit and of the cell respiratory capacity. Antioxid Redox Signal 17: 1–10.

Nagao M, Linden DR, Duenes JA, Sarr MG (2011). Mechanisms of action of the gasotransmitter hydrogen sulfide in modulating contractile activity of longitudinal muscle of rat ileum. J Gastrointest Surg 15: 12–22.

Nagao M, Duenes JA, Sarr MG (2012). Role of hydrogen sulfide as a gasotransmitter in modulating contractile activity of circular muscle of rat jejunum. J Gastrointest Surg 16: 334–343.

Oh ST, Yedidag E, Conklin JL, Martin M, Bielefeldt K (1997). Calcium release from intracellular stores and excitation-contraction coupling in intestinal smooth muscle. J Surg Res 71: 79–86.

Ohba M, Sakamoto Y, Tomita T (1975). The slow wave in the circular muscle of the guinea-pig stomach. J Physiol 253: 505–516.

Ondrias K, Stasko A, Cacanyiova S, Sulova Z, Krizanova O, Kristek F *et al*. (2008). H(2)S and HS(-) donor NaHS releases nitric oxide from nitrosothiols, metal nitrosyl complex, brain homogenate and murine L1210 leukaemia cells. Pflugers Arch 457: 271–279.

Parajuli SP, Choi S, Lee J, Kim YD, Park CG, Kim MY *et al*. (2010). The inhibitory effects of hydrogen sulfide on pacemaker activity of interstitial cells of Cajal from mouse small intestine. Korean J Physiol Pharmacol 14: 83–89.

Pluja L, Fernandez E, Jimenez M (1999). Neural modulation of the cyclic electrical and mechanical activity in the rat colonic circular muscle: putative role of ATP and NO. Br J Pharmacol 126: 883–892.

Pluja L, Alberti E, Fernandez E, Mikkelsen HB, Thuneberg L, Jimenez M (2001). Evidence supporting presence of two pacemakers in rat colon. Am J Physiol Gastrointest Liver Physiol 281: G255–G266.

Pouokam E, Diener M (2011). Mechanisms of actions of hydrogen sulphide on rat distal colonic epithelium. Br J Pharmacol 162: 392–404.

Schicho R, Krueger D, Zeller F, Von Weyhern CW, Frieling T, Kimura H *et al*. (2006). Hydrogen sulfide is a novel prosecretory neuromodulator in the guinea-pig and human colon. Gastroenterology 131: 1542–1552.

Shibuya N, Mikami Y, Kimura Y, Nagahara N, Kimura H (2009a). Vascular endothelium expresses 3-mercaptopyruvate sulfurtransferase and produces hydrogen sulfide. J Biochem 146: 623–626.

Shibuya N, Tanaka M, Yoshida M, Ogasawara Y, Togawa T, Ishii K *et al*. (2009b). 3-Mercaptopyruvate sulfurtransferase produces hydrogen sulfide and bound sulfane sulfur in the brain. Antioxid Redox Signal 11: 703–714.

Strege PR, Bernard CE, Kraichely RE, Mazzone A, Sha L, Beyder A *et al*. (2011). Hydrogen sulfide is a partially redox-independent activator of the human jejunum Na+ channel, Nav1.5. Am J Physiol Gastrointest Liver Physiol 300: G1105–G1114.

Teague B, Asiedu S, Moore PK (2002). The smooth muscle relaxant effect of hydrogen sulphide in vitro: evidence for a physiological role to control intestinal contractility. Br J Pharmacol 137: 139–145.

Wallace JL, Vong L, McKnight W, Dicay M, Martin GR (2009). Endogenous and exogenous hydrogen sulfide promotes resolution of colitis in rats. Gastroenterology 137: 569–578, 578.

Wang R (2002). Two's company, three's a crowd: can H2S be the third endogenous gaseous transmitter? FASEB J 16: 1792–1798.

Zhao P, Huang X, Wang ZY, Qiu ZX, Han YF, Lu HL *et al*. (2009). Dual effect of exogenous hydrogen sulfide on the spontaneous contraction of gastric smooth muscle in guinea-pig. Eur J Pharmacol 616: 223–228.